We are IntechOpen, the world's leading publisher of Open Access books Built by scientists, for scientists

6,900
Open access books available

185,000
International authors and editors

200M
Downloads

Our authors are among the

154
Countries delivered to

TOP 1%
most cited scientists

12.2%
Contributors from top 500 universities



WEB OF SCIENCE™

Selection of our books indexed in the Book Citation Index in Web of Science™ Core Collection (BKCI)

Interested in publishing with us?
Contact book.department@intechopen.com

Numbers displayed above are based on latest data collected.
For more information visit www.intechopen.com



26

Novel Robotic Applications using Adaptable Compliant Actuation. An Implementation Towards Reduction of Energy Consumption for Legged Robots

Björn Verrelst, Bram Vanderborght*
Ronald Van Ham, Pieter Beyl and Dirk Lefeber
Robotics&Multibody Mechanics Research Group
Vrije Universiteit Brussel
Belgium

1. Introduction

Currently, robotics is one of the fields undergoing great scientific innovation and expansion. Automation, via robotic applications, in production industries has grown increasingly. In particular, multifunctional manipulators executing several industrial assembly tasks, i.e. large, fixed-base industrial robots executing "pick-and-place" tasks, with control strategies focused on precision end-effect positioning. Additionally, high precision robotic applications in the framework of medical (surgical) and microchips production are needed especially regarding high precision position control. Electrical motors combined with adapted reduction elements envelop the most commonly used actuator technology at the moment. The developed control algorithms are specifically optimized for position control, possibly in combination with force control. New developments in the area of robotics, however, have currently allowed for the development of multi-legged mobile robots and service robots oriented towards closer human/robot interaction. Especially in Japan, where a large number of corporations each work on a private humanoid robot, strong developments steer towards new applications in social service, domotics, rehabilitation and prosthesis. Important is that these domains require distinct features from the robotic system, such as special dynamical properties for reasons of chock absorption, energy consumption, and flexible and safe human/robot interaction.

Present robots mainly are actuated with electrical drives, with the required reduction units, since this technology is well known. However, the use of these reduction units renders the joint to be more rigid, encompassing several disadvantages vis-à-vis applications of human/robot interactions. In this manner, the structure of the reduction elements is heavily burdened through jolting of highly reflected inertia values. Furthermore, this manner of actuation leaves small room for "soft" robot/human interaction and complicates the exploitation of the system's natural dynamics. The latter encompasses generating robot movements closely associated to the natural, passive movement of the system. However, this requires compliant joints of which ideally stiffness can be manipulated. In a similar way, humans set up their joint stiffness, through relaxation of the muscles, according to the action or task performed. One of the positive consequences of movement within the natural dynamics

Open Access Database www.i-techonline.com

Source: Mobile Robots, Moving Intelligence, ISBN: 3-86611-284-X, Edited by Jonas Buchli, pp. 576, ARS/plV, Germany, December 2006

of the system is the decreased energy consumption, especially important for mobile robots that require an onboard energy source. If the desired movements fall within passive dynamics, certain dynamic limits of the actuator/application frame can moreover shift.
One way to deal with compliance control is by implementing active impedance control using standard electrical actuation. With this kind of control the stiffness is set artificially, but the response time of these systems is fairly low due to several limitations such as sensor resolution, motor control bandwidth, sensor noise, etc…. Moreover, the exploitation of natural dynamics, by means of energy storage in an elastic element, and reduction of shock effects is not possible with such an approach. Reduction of impact effects is essential first for protection with respect to the robot structure itself, e.g. during touch-down impacts of multi-legged robots, and secondly for protection of humans, close to the robot, during unplanned interactions. An alternative for the implementation of compliance control, which tackles the disadvantages previously mentioned, is the use of actuation with inherent mechanical impedance control.
In this context, the "Robotics & Multibody Mechanics" research group of the "Vrije Universiteit Brussel" (VUB) started research, some ten years ago, for alternatives by developing the pleated pneumatic artificial muscle (Daerden et al., 2001). The compressibility of the air in this muscle ensures for the inherent compliance. For a joint driven by two muscles, positioned antagonistically, the joint position can be controlled while adapting compliance. Such muscles are currently being used for the actuation of the biped robot "Lucy" (Verrelst et al., 2005c) and a manipulator arm with direct human/robot interaction (Van Damme et al., 2005), and will be used to power a semi-active ankle foot prosthesis and an exosceleton for the lower extremities to assist during rehabilitation of paraplegic patients. These experimental setups are under study to develop specific control strategies for steering a robot with compliant joints, and more specifically adaptive compliance. In this framework, the robot "Lucy" is steered through trajectory control in the joints in combination with exploitation of the natural dynamics of the robot system, using the adaptive compliance characteristic of the actuators.
This publication will report on the implementation of compliant actuation in the biped "Lucy" and a one degree of freedom pendulum setup, focusing on the reduction of energy consumption by exploitation of natural dynamics. In the current state of this research the tracking control strategies developed for the compliant actuators allow the biped to walk continuously at moderate speeds while changing walking speed and step length. The control strategy to combine compliance setting with trajectory control, influencing the eigenfrequency of the system, so far has been successfully implemented in a reduced configuration such as an experimental pendulum setup actuated by one antagonistic pair of two artificial muscles.
First an overview is given on the research of legged robots in combination with exploitation of natural dynamics, followed by an overview of existing variable compliant actuation systems . Next, a description of the pleated pneumatic artificial muscle, which is the present choice to implement adaptable compliance, is given. Subsequently, the low-level control strategies allowing both position and compliance control in an antagonistic setup of two such artificial muscles are described. The implementation of these control strategies in a one degree of freedom pendulum structure is the main subject, for which the reduction of energy consumption is shown by experimental results. Finally, the extension of the tracking control to the complete biped is discussed briefly and its experimental validation on joint trajectory tracking for continuous walking of the biped "Lucy" on a treadmill is given.

1.1 Legged Locomotion and Natural Dynamics

Legged locomotion can be classified in terms of their overall control strategy. The more recent robots are dynamically balanced machines, whereas the older machines were statically balanced. Statically balanced robots keep the centre of mass within the polygon of support in order to maintain postural stability. To avoid inertial effects these machines move rather slow, contrary to dynamically balanced robots where the inertial effects are taken into account in the different control strategies. When the control unit not only takes these inertial effects into account but also exploits them, the term natural dynamics arises.

Natural dynamics or passive dynamics is the unforced response of a system under a set of initial conditions. In general, for legged locomotion these natural dynamics are not or only partially exploited. Examples of exploitation of the natural dynamics are the swing-leg swinging freely without hip actuation or the body and stance-leg pivoting as an inverted pendulum around an un-actuated ankle. Legged systems that walk completely without actuation are the so called "Passive Walkers". These machines are only powered by gravity and they are mechanically tuned in order to walk down a sloped surface. These "Passive Walkers" could be pointed out as very energy efficient but unfortunately they are of little practical use. A minimum actuation should be provided to walk on level ground to overcome friction and impact losses. Anyway, it is important to exploit the natural dynamics by trying to incorporate the unforced motion of a system instead of ignoring or avoiding it. Doing so could positively affect energy consumption and control efforts.

One of the first to incorporate passive dynamics for legged locomotion was Matsuoka (Matsuoka, 1980) and later Raibert (Raibert, 1986). The latter became one of the pioneers in dynamic walking with his several one or more legged hopping robots. For these systems he used a pneumatic spring in the telescopic legs to influence and exploit the passive dynamics in the vertical direction. Exploiting passive dynamics by means of the stance leg pivoting freely as an inverted pendulum was incorporated in the biped walkers of Takanishi (Takanishi, 1985), Lee and Liao (Lee et al., 1988). At the end of the eighties Thompson and Raibert (Thompson et al., 1989) studied the additional exploitation of natural dynamics of the hip motion by placing a torsional spring. At the same time McGeer (McGeer, 1990) built and studied a passive walker without compliant elements. Later he analysed theoretically and by means of simulation walkers with hip compliance but with the body being a point-mass. During the nineties the group of Andy Ruina (1998) (Garcia et al., 1998) studied in more detail the models of McGeer and extended the two dimensional model to three dimensions while building several Passive Walkers. In the second half of the nineties the group of Buehler (Gregorio et al, 1997) built a legged hopping monoped following the examples of Raibert using electrical actuation combined with a torsional spring in the hip and a linear spring in the telescopic leg. The control strategy was to calculate the passive dynamic trajectories with the correct initial conditions as a function of the desired forward speed while in parallel with these trajectories standard active control was used to cope with imperfections of the modelling of the passive dynamics. A more intuitive control but still focussing on exploiting natural dynamics was done at MIT by Pratt making use of the "Series Elastic Actuators" (Pratt et al., 1995) in the two legged robot "Spring Flamingo" (Pratt et al., 1998). After 2000, Quartet III was built (Osuka et al., 2000), this quadruped starts walking down a sloped surface in an active way and gradually decreases control input to transfer to passive walking. Asano and Yamakita introduced the "virtual gravity field" (Asano et al., 2000) for horizontal walking in order to exhibit virtual passive walking based

on McGeers models but with hip and ankle actuation. Wisse and van der Linde (Wisse et al., 2001) studied a 3D Passive Walker with a pelvic body at the university of Delft.
Most of these models use only the inertial properties to determine the eigenfrequency and additionally fixed compliance of mechanical linear or rotational springs. As a result the eigenfrequency of these systems is set during construction which limits the different passive walking patterns and walking speeds. Flexibility, with the ability to change this natural frequency, is increased by implementing passive elements with variable compliance. In this context the group of Takanishi developed the two-legged walker WL-14 (Yamagushi, 1998), where a complex non-linear spring mechanism makes changes in stiffness possible. A more elegant way to implement variable compliance is to use pneumatic artificial muscles in an antagonistic setup, where the applied pressures determine stiffness. Research on this topic was done by Van der Linde (van der Linde, 1998), Wisse (Wisse, 2001) and Caldwell (Davis et al., 2001) by implementation of McKibben muscles.

1.2 Variable Compliance Actuators

An important contribution in the research towards soft actuators has been given by Pratt with the development of the "series elastic actuator" (Pratt et al., 1995). It consists of a motor drive in series with a spring. The disadvantage of such a setup is that the stiffness can not be changed. Nowadays, more and more research is performed to make the compliance of the actuator adaptable. The Robotics Institute at Carnegie Mellon University developed the "Actuator with Mechanically Adjustable Series Compliance" (AMASC) (Hurst et al., 2004). It has fibreglass springs with a large energy storage capacity. The mechanism has two motors, one for moving the position and the other for controlling the stiffness. However the mechanism is so complex and heavy that it can't be used in mobile robots. The novel electro-mechanical "Variable Stiffness Actuation" (VSA) motor (Bicchi et al., 2004) of the university of Pisa has been designed for safe and fast physical human/robot interaction. A timing transmission belt connects nonlinearly the main shaft to an antagonistic pair of actuator pulleys connected to position-controlled back-drivable DC motors. The belt is tensioned by springs. Concordant angular variations control displacements of the main shaft, while the opposite variations of the two DC motors generate stiffness variations. The "Biologically Inspired Joint Stiffness Control" (Migliore et al.,2005) can be described as two antagonistic coupled Series Elastic Actuators, where the springs are made non-linear. At Northwestern University the "Moment arm Adjustment for Remote Induction Of Net Effective Torque" (MARIONET) (Sulzer et al., 2005) actuator has been developed. This rotational joint uses cables and transmission to vary the moment arm such that the compliance and equilibrium position is controllable. Special is that this device doesn't use an elastic element, the system moves against a conservative force field created by a tensioner. Hollander and Suger (Hollander, 2004) describe several variable stiffness systems by changing the "effective" structure of spring elements. One of them uses a spring leave of which the active length is changed by an extra actuator. This principle has also been used for the "Mechanical Impedance Adjuster" (Morita et al., 1995) developed at the Sugano Lab. And a complete 3D joint with variable compliance, by using only 2 motors, has been developed (Okada et al., 2001) for a shoulder mechanism, but the compliances of the different DoF's are coupled. Another recent approach is the MACCEPPA actuator (Van Ham et al., 2005) which uses two motors and only one spring element. The compliance and rest position of the actuator can be set independently, each by a separate motor, due to a specific geometric positioning of the spring. Finally, as already mentioned in the previous section, variable compliance can be

achieved with pneumatic artificial muscles in an antagonistic setup. In fact, any non-linear compliant element in an antagonistic setup will do for this purpose, but artificial muscles provide an elegant and compact solution.

2. Pleated Pneumatic Artificial Muscle

2.1 Force Characteristic

A pneumatic artificial muscle is essentially a membrane that will expand radially and contract axially when inflated, while generating high pulling forces along the longitudinal axis. Different designs have been developed. The best known is the so called McKibben muscle (Schulte, 1961). This muscle contains a rubber tube which expands when inflated, while a surrounding netting transfers tension. Hysteresis, due to dry friction between the netting and the rubber tube, makes control of such a device rather complicated. Typical for this type of muscle is a threshold level of pressure before any action can take place. The main goal of the new design (Daerden et al., 2001) was to avoid friction, thus making control easier while avoiding the threshold. This was achieved by arranging the membrane into radially laid out folds that can unfurl free of radial stress when inflated. Tension is transferred by stiff longitudinal fibres that are positioned at the bottom of each crease.



Fig. 1. Pleated Pneumatic Artificial Muscles at 3 different contraction levels.

A photograph of the inflated and deflated state of the Pleated Pneumatic Artificial Muscle (PPAM) is given in Fig. 1. If we omit the influence of elasticity of the high tensile strength material used for the fibres, the characteristic for the generated force is given by:

$$F = pl^2 f(\varepsilon, R/l) \tag{1}$$

where p is the applied gauge pressure, l the muscle's full length, R its unloaded radius and ε the contraction. The dimensionless function f, which depends only on contraction and geometry, is given for different values of broadness R/l on the left graph of Fig. 2.

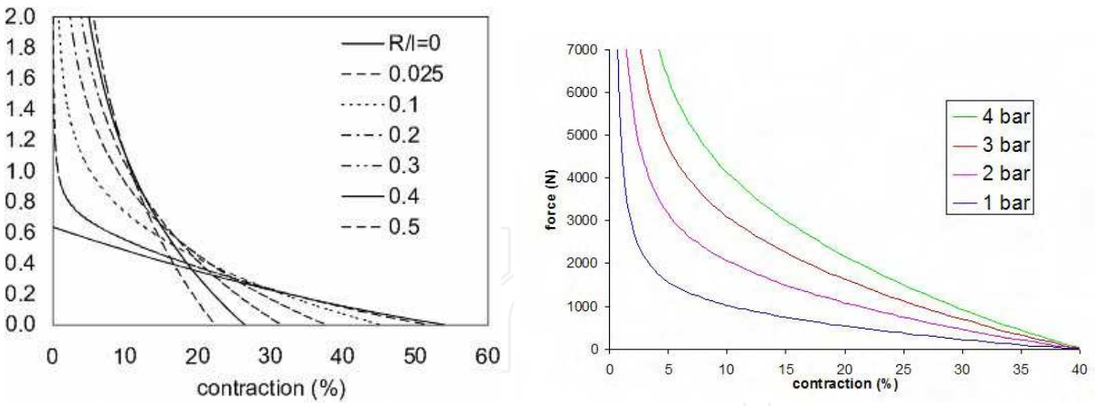


Fig. 2. (left) Dimensionless force function for different broadness ; (right) Generated force of a muscle with initial length 11cm and unloaded diameter 2.5cm.

The thicker the muscle, the less it contracts and the higher the forces it generates. Contraction can reach up to 54% in a theoretical case with *R/l=0*. At low contraction forces are extremely high causing excessive material loading, and the generated forces drop too low for large contraction. Thus contraction is bounded between two limits, 5 and 35%, in practise. The graph on the right of Fig. 2 gives the generated force for different pressures of a muscle with initial length 11cm and unloaded diameter 2.5cm. Forces up to 5000N can be generated with gauge pressure of only 3bar while the device weighs about 100g.

2.2 Antagonistic Muscle Setup: Generated Torque

Pneumatic artificial muscles can only pull. In order to have a bi-directionally working revolute joint one has to couple two muscles antagonistically. The muscle connections -pull rods and lever mechanism- are designed such that the muscle's highly non-linear force-length characteristic is transformed to a more flattened torque-angle characteristic.
The left picture of Fig. 3 shows the straightforward connecting principle.

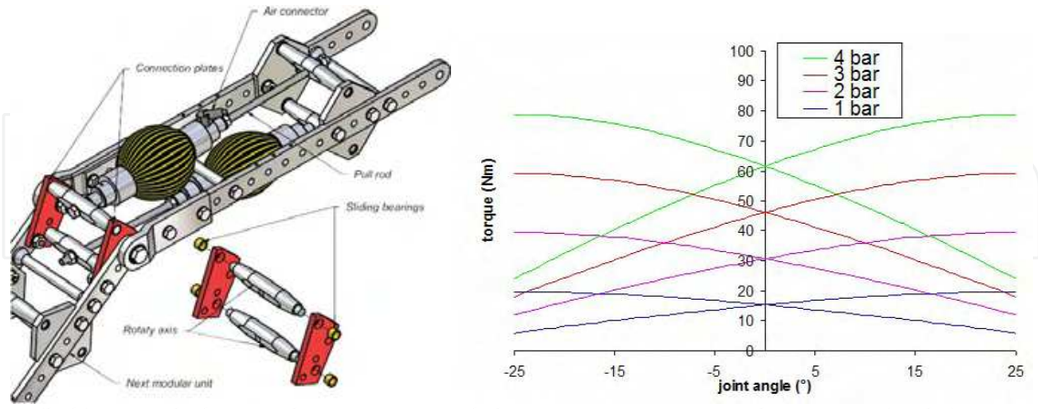


Fig. 3. (left) straightforward connection of the antagonistic muscle setup ; (right) generated torques by each muscle of an antagonistic setup at different pressure levels.

Depending on the desired function of the joint, the dimensions can be chosen in order to meet the needs of the specified joint function, not only in torque levels but also in range of motion. The torque characteristics of the pendulum (discussed below) are shown on the right of Fig. 3. Both torques are given for different pressure values. Taking into account

equation (1) and if r_1 and r_2 define the leverage arm of the agonist and antagonist muscle respectively, the joint torque (T) is given by following expression

$$T = T_1 - T_2 = p_1 l_1^2 r_1 f_1 - p_2 l_2^2 r_2 f_2 = p_1 t_1(\theta) - p_2 t_2(\theta) \tag{2}$$

with p_1 and p_2 the applied gauge pressures in agonist and antagonist muscles respectively which have lengths l_1 and l_2. The dimensionless force functions of both muscles are given by f_1 and f_2. The functions t_1 and t_2, in equation (2), are determined by the choices made during the design phase and depend on the joint angle θ. Thus joint position is influenced by weighted differences in gauge pressures of both muscles.

2.3 Antagonistic Muscle Setup: Compliance

The PPAM has two sources of compliance: gas compressibility and the dropping force to contraction characteristic. The latter effect is typical for pneumatic artificial muscles while the first is similar to standard pneumatic cylinders. Joint stiffness, the inverse of compliance, for the considered revolute joint can be obtained by the angular derivative of the torque characteristic in equation (2):

$$K = \frac{dT}{d\theta} = \frac{dp_1}{d\theta} t_1 + p_1 \frac{dt_1}{d\theta} - \frac{dp_2}{d\theta} t_2 - p_2 \frac{dt_2}{d\theta} \tag{3}$$

The terms $dp_i/d\theta$ represent the share in stiffness of changing pressure with contraction, which is determined by the action of the valves controlling the joint and by the thermodynamic processes taking place. If the valves are closed and if we assume polytropic compression/expansion the pressure changes inside the muscle are a function of volume changes:

$$P_i V_i^n = P_{i_0} V_{i_0}^n \text{ with } P_i = p_i + P_{atm} \tag{4}$$

leading to:

$$\frac{\mathrm{d}p_i}{\mathrm{d}\theta} = -n(P_{atm} + p_{i_0}) \frac{V_{i_0}^n}{V_i^{n+1}} \frac{dV_i}{d\theta} \tag{5}$$

With P_i, V_i the absolute pressure and volume of muscle i, P_{io} the absolute initial pressure, V_{io} the initial volume when muscle i was closed and p_i, p_{io} the gauge pressure and initial gauge pressure. n is the polytropic index and P_{atm} the atmospheric pressure.

Taking the torque characteristics as an example the following reasoning can be made for closed muscles. An increase of the angle θ results in an increase of the torque generated by the extensor muscle (see right Fig. 3) while its volume decreases (expanded muscles have lower torques). Thus $dt_1/d\theta > 0$ and $dV_1/d\theta < 0$. For the flexor muscle the actions will be opposite. Combining equations (3), (4) and (5) with this information gives:

$$K = k_1 p_{1_0} + k_2 p_{2_0} + k_{atm} P_{atm} \tag{6}$$

with:

$$\begin{aligned} k_i &= n t_i \frac{V_{i_0}^n}{V_i^{n+1}} \left| \frac{dV_i}{d\theta} \right| + \frac{V_{i_0}^n}{V_i^n} \left| \frac{dt_i}{d\theta} \right| > 0 \qquad i = 1,2 \\ k_{atm} &= k_1 + k_2 - \left| \frac{dt_1}{d\theta} \right| - \left| \frac{dt_2}{d\theta} \right| \end{aligned} \tag{7}$$

The coefficients k_1, k_2, k_{atm} are a function of the angle and are determined by the geometry parameters of the joint and muscles. From equation (6) the conclusion is drawn that a passive spring element is created with an adaptable stiffness controlled by the weighted sum of both initial gauge pressures when closing the muscle. Since stiffness is depending on a sum of gauge pressures while position is determined by differences in gauge pressure, the angular position can be controlled while setting stiffness.

3. Trajectory control with adaptable compliance

In this section the proposed strategy of combining adaptable passive behaviour with trajectory control is illustrated. The control architecture consists of two parts: the joint trajectory tracking controller which calculates the necessary torque to track a desired trajectory and the compliance controller to reduce energy consumption and control efforts.

3.1 Joint Trajectory Tracking Controller

This paragraph discusses the joint trajectory tracking controller of which the separate units are depicted in Fig. 4. The tracking controller is divided into a computed torque controller, a delta-p unit and a pressure bang-bang controller. The computed torque controller calculates the required joint torque based on the pendulum dynamics. The delta-p unit translates these calculated torques into desired pressure levels for the two muscles of the antagonistic set-up. Finally the bang-bang pressure controller determines the necessary valve actions to set the correct pressures in the muscles. In the next sections the different elements of the control structure are discussed in more detail.

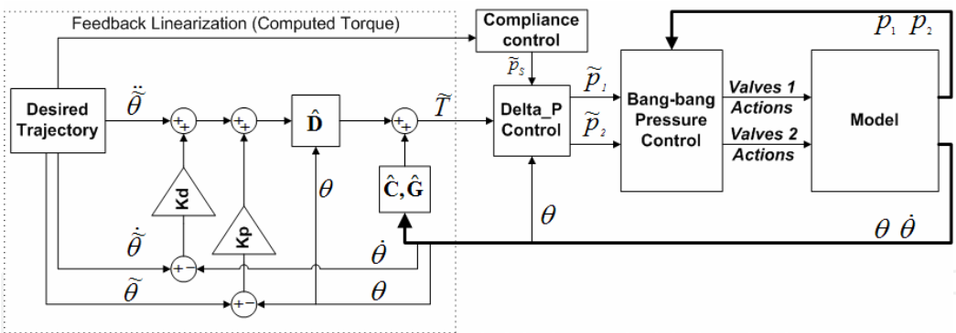


Fig. 4. Trajectory tracking control scheme.

3.1.1 Computed Torque

In the first module, the joint torques are calculated using the popular computed torque technique consisting of a feedforward part and a PID feedback loop. This results in the following calculation:

$$\tilde{T} = C_e(\theta,\dot{\theta})\dot{\theta} + G_e(\theta) + D_e(\theta)\left(\ddot{\tilde{\theta}} - K_P(\theta - \tilde{\theta}) - K_I\sum(\theta - \tilde{\theta}) - K_D(\dot{\theta} - \dot{\tilde{\theta}})\right) \tag{8}$$

The parameters D_e, C_e and G_e contain the estimated values of the inertia, centrifugal and gravitational parameters of the system under study. The feedback parameters K_p, K_i and K_d are manually tuned.

3.1.2 Delta-p Unit

The computed torque $\tilde{T}$ is fed to the delta-p control unit, which calculates the required pressure values to be set in the muscles. These two gauge pressures are generated as follows:

$$\tilde{p}_1 = \frac{\tilde{p}_S}{\hat{t}_1(\theta)} + \Delta\tilde{p} \tag{9a}$$

$$\tilde{p}_2 = \frac{\tilde{p}_S}{\hat{t}_2(\theta)} - \Delta\tilde{p} \tag{9b}$$

with p_s a parameter that is used to influence the sum of pressures and consequently the joint stiffness and $\Delta\tilde{p}$ a parameter that influences the difference in pressure of the two muscles in order to control the generated torque. The functions $\hat{t}_i(\theta)$ *(i=1,2)* represent the torque characteristics of the antagonistic muscle setup and are calculated with estimated values of the muscle force functions and geometrical parameters. Expression (2) allows to link the required torque to the required pressure values in the muscles:

$$\tilde{T} = \tilde{p}_1\hat{t}_1(\theta) - \tilde{p}_2\hat{t}_2(\theta) = (\hat{t}_1(\theta) + \hat{t}_2(\theta))\Delta\tilde{p} \tag{10}$$

If the calculated pressure values $\tilde{p}_i$ *(i=1,2)* of equations (9) are set in the muscles, the generated torque depends only on $\Delta\tilde{p}$ and is independent of the joint stiffness parameter p_s, in case the modelling would be perfect. This means that joint stiffness is changed without affecting the joint angular position. Feeding back the knee angle θ and introducing the torque $\tilde{T}$, expression (10) can be used to determine the required $\Delta\tilde{p}$:

$$\Delta\tilde{p} = \frac{\tilde{T}}{\hat{t}_1(\theta) + \hat{t}_2(\theta)} \tag{11}$$

The delta-p unit is actually a feedforward calculation from torque level to pressure level, using the kinematic model of the muscle actuation system. The calculated $\Delta\tilde{p}$ affects the torque required to track the desired trajectory, while p_s is introduced to determine the sum of pressures which influences the stiffness of the joint which will be discussed in section 3.2.

3.1.3 Bang-bang Pressure Controller

The weight of the valves controlling the muscles should be taken as low as possible. But since most pneumatic systems are designed for fixed automation purposes where weight is not an issue at all, most off-the-shelf proportional valves are far too heavy for this application. Thus a proper design of the pressure control is of great importance. In order to realize a lightweight rapid and accurate pressure control, fast switching on-off valves are used. The pneumatic solenoid valve '821 2/2 NC' made by Matrix weighs only 25g. With their reported opening times of about 1ms and flow rate of 180 Stdl/min, they are about the fastest switching valves of that flow rate currently available.

To pressurize and depressurize the muscles, which have a varying volume up to 400ml, a number of these small on-off valves are placed in parallel. Obviously the more valves used the higher the electric power consumption, the price and also the weight will be. Simulations of the pressure control of a constant volume resulted in a choice of two inlet and four outlet valves. The different number between inlet and outlet comes from the asymmetric pressure conditions between inlet and outlet, combined with the aim to create equal muscle's inflation and deflation times.

To connect the 6 valves into one compact pressure regulating valve, two special collectors were designed. These collectors replace the original aluminium connector plates of the valves, resulting in a weight of the complete pressure regulating valve of about 150gr. The left of Fig. 5 shows a picture of the pressure valves with their speed-up circuit. The speed-up circuit reduces opening and closing times of the valves. The pressure control in a volume is achieved with a bang-bang controller with various reaction levels depending on the difference between measured and desired pressure (right of Fig.5.). If this difference is large, two inlet or four outlet valves, depending on the sign of the error, are opened. If this difference is small, only one valve is switched and when the error is within reasonable limits no action is taken, leaving the muscle closed. More detailed information on the valve system can be found in the work of Van Ham (Van Ham et al., 2005).

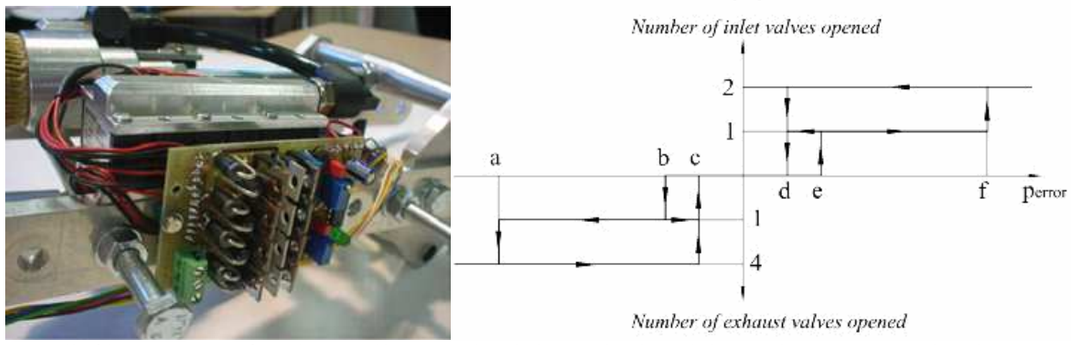


Fig. 5. (left) Picture of valve collector; (right) Multi-level bang-bang control scheme with dead zone (a = -60, b = -25, c = -20, d = 20, e = 25, f = 60 mbar).

3.2 Compliance Controller

In this section a strategy to calculate an appropriate value of p_s is described. The idea is to fit the natural compliance with the required ones. The desired stiffness related to the desired trajectory $\tilde{K}^{Traj}$, the inverse of the compliance, is calculated as the derivative of the torque $\tilde{T}$, required to track the trajectory, with respect to the desired joint angle $\tilde{\theta}$. The torque $\tilde{T}$ is found by inverse dynamics.

$$\tilde{K}^{Traj} = \frac{d\tilde{T}}{d\tilde{\theta}} = \frac{d}{d\tilde{\theta}}\left(D_e\left(\tilde{\theta}\right)\ddot{\tilde{\theta}} + C_e\left(\tilde{\theta},\dot{\tilde{\theta}}\right)\dot{\tilde{\theta}} + G_e\left(\tilde{\theta}\right)\right) \tag{12}$$

The natural actuator stiffness K^{Act} can be found by deriving equation (10) with respect to the desired joint angle $\tilde{\theta}$:

$$K^{Act} = \frac{d\tilde{p}_1}{d\tilde{\theta}}\hat{t}_1 + \tilde{p}_1\frac{d\hat{t}_1}{d\tilde{\theta}} - \frac{d\tilde{p}_2}{d\tilde{\theta}}\hat{t}_2 - \tilde{p}_2\frac{d\hat{t}_2}{d\tilde{\theta}} \tag{13}$$

The required pressure slopes are a combination of equation (5), valid for closed muscles, with equations (9), in which the initial pressure p_{i_0} is set equal to $\tilde{p}_i$:

$$\frac{d\tilde{p}_i}{d\tilde{\theta}} = -\left[\frac{\tilde{p}_S}{\hat{t}_i} + \left(P_{atm} + (-1)^{i+1}\Delta p\right)\right]\left(n\frac{\hat{V}_{i_0}^{\,n}}{\hat{V}_i^{\,n+1}}\frac{d\hat{V}_i}{d\tilde{\theta}}\right) \qquad i = 1,2 \tag{14}$$

Combining equations (13) and (14) while setting expected actuator stiffness K^{Act} equal to the desired stiffness $\tilde{K}^{Traj}$, the optimal actuator stiffness parameter $\tilde{p}_S^{Opt}$ can be calculated:

$$\tilde{p}_S^{Opt} = \frac{K^{Traj} - \Delta\tilde{p}A - P_{atm}B}{C} \tag{15}$$

with:

$$A = -\frac{n\hat{t}_1}{\hat{V}_1}\frac{d\hat{V}_1}{d\tilde{\theta}} - \frac{n\hat{t}_2}{\hat{V}_2}\frac{d\hat{V}_2}{d\tilde{\theta}} + \frac{d\hat{t}_1}{d\tilde{\theta}} + \frac{d\hat{t}_2}{d\tilde{\theta}} \tag{16a}$$

$$B = -\frac{n\hat{t}_1}{\hat{V}_1}\frac{d\hat{V}_1}{d\tilde{\theta}} + \frac{n\hat{t}_2}{\hat{V}_2}\frac{d\hat{V}_2}{d\tilde{\theta}} \tag{16b}$$

$$C = -\frac{n}{\hat{V}_1}\frac{d\hat{V}_1}{d\tilde{\theta}} + \frac{n}{\hat{V}_2}\frac{d\hat{V}_2}{d\tilde{\theta}} + \frac{1}{\hat{t}_1}\frac{d\hat{t}_1}{d\tilde{\theta}} - \frac{1}{\hat{t}_2}\frac{d\hat{t}_2}{d\tilde{\theta}} \tag{16c}$$

Note that the initial volume V_{i_0} when closing a muscle, is set equal to the actual volume V_i, analogously as for the pressure. Using the value $\tilde{p}_S^{Opt}$ in the calculation of the control variables in equations (9) reduces the energy consumption. However, there still exists a strong dependence on the controller parameters, such as bang-bang pressure control reaction levels and feedback gains of the computed torque controller. E.g. decreasing the reaction levels of the bang-bang controller for opening a valve would increase valve switching, due to the delay time of the valves.

4. Simulation and Experimental Results

In this section the proposed compliance controller in combination with the trajectory tracking controller is discussed both through simulations and experiments on a physical pendulum setup. This single pendulum, driving a load at its endpoint, is actuated by one antagonistic pair of artificial muscles as described in section 2.2.

4.1 Calculation of Energy Consumption

The energy consumption for compressed air depends not only on the air mass flows but is related to the thermodynamic conditions of the compressed air supply source. One way to give an idea of energy consumption is to calculate the exergy associated with the particular pneumatic air mass flow. Exergy is in fact the maximum amount of energy, with respect to the surrounding environment, which can be transformed into useful work. For example, the air mass flow entering the muscle system comes from a compressed air reservoir at certain temperature and pressure level. The surrounding environment is regarded as the atmosphere. The exergy of the pneumatic power supply is then calculated as the minimal work needed to compress the atmospheric air to the pressure supply conditions. For a compressor, the minimal work needed to compress air from pressure level p_{atm} to p_1 is done at isothermal conditions and can be calculated as follows (Rogers et al., 1992):

$$\dot{W}_{isotherm} = \dot{m}_{air} r T_{atm} \ln\frac{p_1}{p_{atm}} \tag{17}$$

hereby assuming the air to behave as a perfect gas. The symbol $\dot{m}_{air}$ represents the total air mass flowing through the compressor, r is the dry air gas constant and T_{atm} is the temperature of the atmosphere expressed in Kelvin. The absolute supply pressure level is set at 7bar, the atmospheric absolute pressure at 1bar and the atmospheric temperature is 293K. This is just

one way to calculate the energy consumption. The absolute energy consumption is not the most important aspect, however. It is the reduction of the energy consumption that one can achieve, when matching system and trajectory compliances, which is the main focus.

4.2 Simulation Results

4.2.1 Simulator

Most parts of the system are highly non-linear: force/torque-contraction of the muscles, the thermodynamic processes, the mechanical load of the pendulum, the pressurized air flows through the discrete number of valves,... which makes it difficult to perform stability/convergence analysis. In order to evaluate the proposed control strategy while taking into account non-linearity, a hybrid simulator was created, meaning that both the pneumatics and mechanics are put together in one dynamic simulation model. The pressure variation inside the muscle is represented by first order differential equations deduced from the first law of thermodynamics for an open system while assuming a perfect gas for the compressed air. The orifice valve flows are derived from the model presented by ISO6358 standard (International Standard, 1998). The integration of these first order differential equations coupled with the mechanical differential equations of the pendulum and the muscle torque/contraction characteristics results in the calculated torques. Doing so includes the muscle actuator characteristics, which allows the limitations in the motion of the pendulum to be studied. Detailed information on the simulation model can be found in (Verrelst, 2005a) for a one degree of freedom setup and in (Verrelst, 2005b) for the complete biped, elaborated on in section 5. To test the robustness, model parameter uncertainties are introduced in the simulation model, e.g. 5% on the mass and CoG (Centre of Gravity), 10% on the inertia and 5% on both force functions of the antagonistic set-up. A time delay of 1ms for closing and opening of the valves and a sampling time of 2ms of the controllers are regarded.

4.2.2 Results and discussion

To evaluate the proposed control architecture a sinusoidal trajectory is imposed with a linearly increasing frequency from 1.5 Hz to 2 Hz (chirp function). Due to the increasing frequency the stiffness has to be adapted continuously. To show the effectiveness of the proposed compliance controller the results of an optimal p_S^{Opt} as calculated with equation (15) have been compared with the results obtained with some deviations on it: $p_S = 1.5 p_S^{Opt}$ and $p_S = 0.5 p_S^{Opt}$. The influence of the parameter p_S on the exergy consumption and mean angle tracking error is given in Table 1. This shows that tracking the desired trajectory with p_S^{Opt} consumes less energy, up to 6 times less than the considered deviated states (in simulation), while the tracking error is not deteriorated.

p_S	**Exergy consumption (J)**	**Mean angle error (°)**
$p_S = 0.5 p_S^{Opt}$	5.28	0.09
$p_S = p_S^{Opt}$	0.87	0.064
$p_S = 1.5 p_S^{Opt}$	5.63	0.122

Table 1. Exergy consumption and mean angle error for different p_s values.

The effect of choosing the optimal p_S^{Opt} can also be seen in the graphs of Fig. 6. These graphs show the valve actions taken by the bang-bang pressure controller. Note that in these figures closed valves are represented by a horizontal line depicted at respectively 1.5, 2.0 and 2.6bar pressure level, while a small peak upwards represents one opened inlet valve, a small peak downwards one opened exhaust valve.

The number of valve actions is significantly lower when the compliance setting is at the optimal value. On the right, the desired and actual pressures are depicted. In the optimal case the desired pressure is nearly the natural pressure already present in the muscle. Only at certain instants a little energy input has to be provided to the system in order to increase the swing frequency. In the cases where the compliance setting is not optimal, significantly more valve switching is required. The imposed trajectory differs substantially from the natural movement of the pendulum causing a lot of valve switching and consequently energy dissipation. The actual motion, however, is the same because it is controlled by the joint trajectory tracking controller.

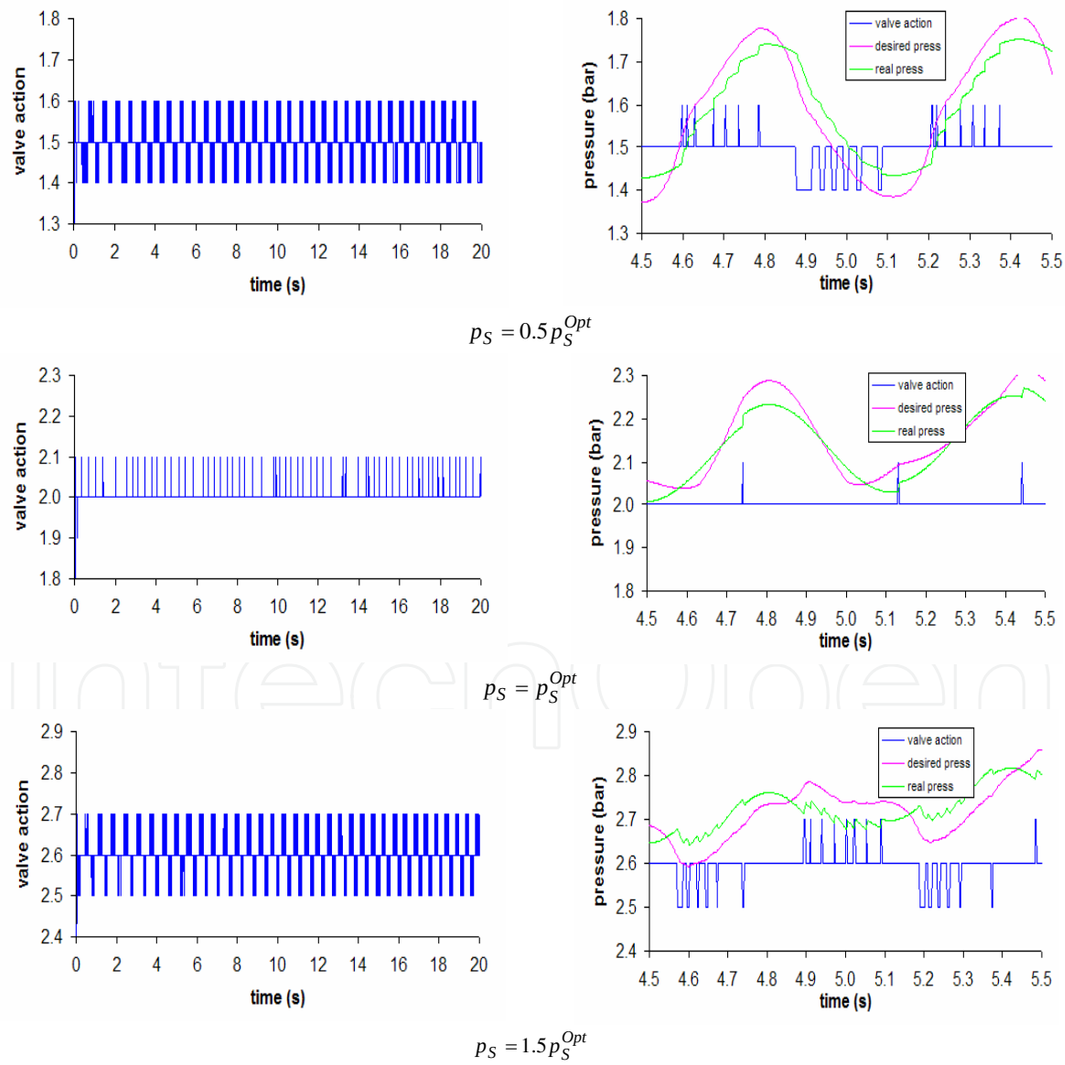


Fig. 6. Valve action and detail of the pressure changes for the 3 different settings of p_s.

4.3 Experimental Results with a single DoF Pendulum

4.3.1 Pendulum

The complete set-up of the pendulum is shown in Fig. 7. The structure is made of a high-grade aluminium alloy, AlSiMg1, and the design is exactly the same as the limbs of the robot "Lucy" (see section 5), only the connection parameters of the pull rod and lever mechanism are specific. The actual length of the swinging part of the pendulum is 45cm, and a weight of 10kg is attached at the end.

The sensors are Agilent HEDM6540 incremental encoder for reading the joint position and two pressure sensors (Honeywell CPC100AFC), mounted inside each muscle. The controller is implemented on a PC and a National Instruments (AT-MIO-16E-10) is used for data acquisition, sampling at 500Hz.

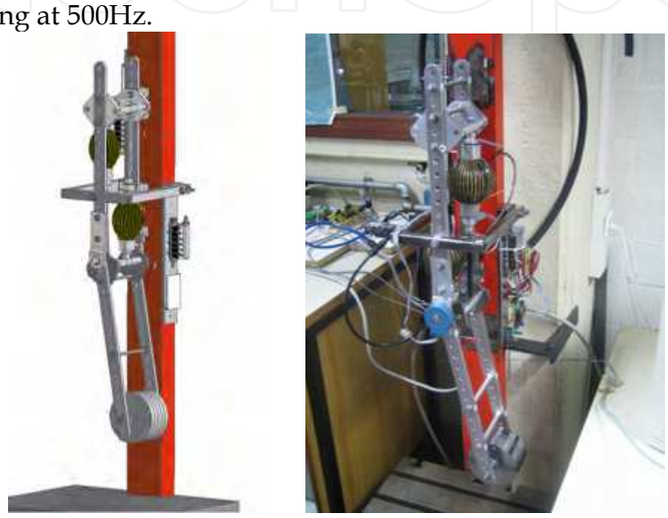
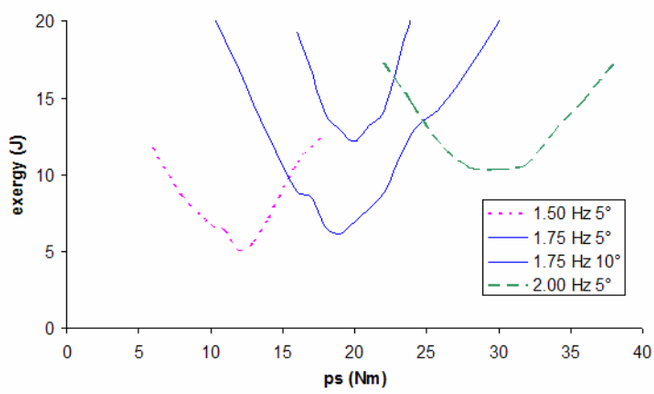


Fig. 7. CAD drawing and photograph of the pendulum setup.

4.3.2 Results and Discussion

Fig. 8 shows the total experimentally determined exergy as a function of the parameter p_s for pure sinusoidal trajectories with different frequencies and amplitudes. The graphs show that an optimal p_s value exist for each frequency and, as expected, this optimal value increases with the frequencies.



	$P_{S_{\exp}}^{Opt}$ (Nm)	$P_{S_{calc}}^{Opt}$ (Nm)
1.50 Hz	12	12.6
1.75 Hz	19	21.4
2.00 Hz	30	31.7

Fig. 8. (Left) Total output exergy vs stiffness parameter p_s for different frequencies and amplitudes; (Right) Optimal p_s values of the graph compared with calculated ones.

On the right of Fig. 8, both the experimentally determined ($P_{S_{exp}}^{Opt}$) and calculated ($P_{S_{calc}}^{Opt}$; equation (15)) optimal values of $p_{s,}$ for the three different swing frequencies of the graph on the left of Fig. 8, are given. The calculated optimal p_s gives a good approximation of the compliance parameter that is required for minimal energy consumption in the experiment. The graph of Fig. 8 additionally shows the total exergy as a function of the parameter p_s for two amplitudes of 5° and 10° at 1.75Hz. The optimal stiffness stays nearly the same as we would expect for a pendulum, but energy consumption is higher for larger amplitudes. The actual passive trajectory of the pendulum deviates from a pure sine-wave. This deviation increases for larger amplitudes. Consequently, more valve switching is needed for larger movements, which induces higher energy consumption.

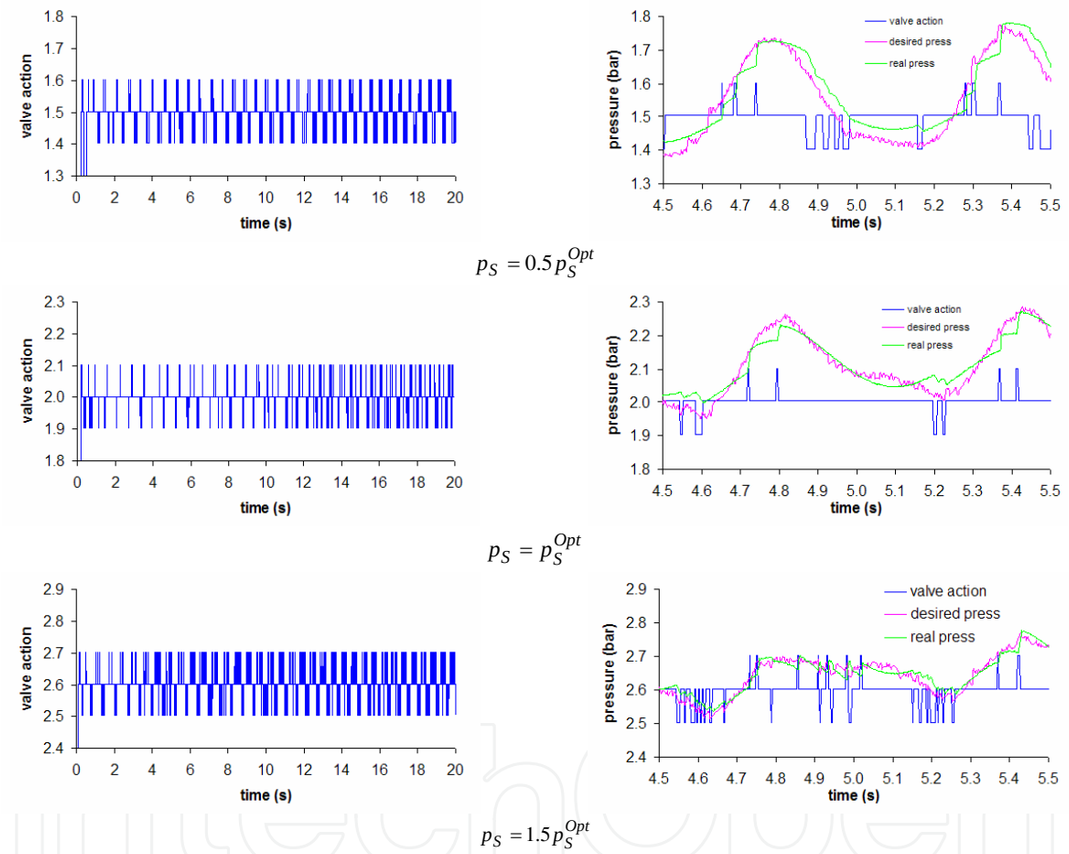


Fig. 9. Experimentally determined valve action and detail of the pressure changes for 3 different settings of p_s.

To test the effectiveness of the proposed compliance controller the same experiment with the chirp function trajectory going from 1.5Hz to 2.0Hz, as in simulation (section 4.2.2), is performed on the real pendulum. Graphs depicting valve action and detailed pressure courses are given in Fig. 9. One can see that the results are comparable to the simulations shown in Fig. 6. The fact that there are more valve actions in reality than in simulation can be explained by some leakages in the muscles and deviations due to parameter estimation errors. The desired pressure slopes are not as smooth as in simulation, this is mainly due to the noise on the input signal, most of it coming from the velocity part of the PID controller. For more complex trajectories than a sine function the consumed energy will increase, because the imposed

trajectory differs more with respect to the natural movement of the pendulum, which is a sine function for small angles. The study of the sine wave is however of great importance for bipedal locomotion. The energy transfer mechanism used in walking is often referred to as an ``inverted pendulum mechanism''. This observation has led to the development of the so called ``passive walkers'' where walking is a succession of swing motions.

5. Bipedal Robot "Lucy"

5.1 Robot Hardware

The Multibody Mechanics Research Group of the Vrije Universiteit Brussel has built the planar walking biped "Lucy". The goal of the project is to achieve a lightweight bipedal robot able to walk in a dynamically stable way, while exploiting the passive behaviour of the PPAM's in order to reduce energy consumption and control efforts. In primary instance the compressor or supply tank and PC are placed outside the robot for simplicity reasons. Building an autonomous robot is not the major issue, the main focus of the research is to investigate joint compliance variation for bipedal walking mechanims. The muscles are however strong enough to carry an additional payload.

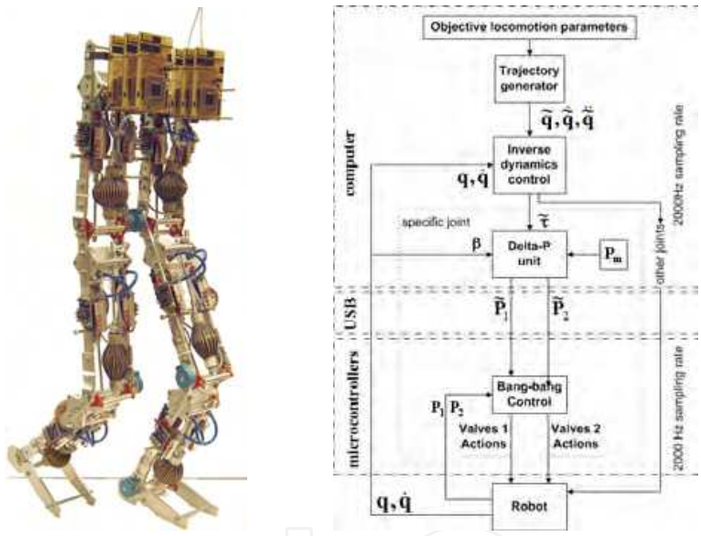


Fig. 10. (left) The robot "Lucy" ; (right) Control scheme for the complete robot.

The left of Fig. 10 shows the robot "Lucy" which weighs about 30kg and is 150cm tall. The motion of "Lucy" is restricted to the sagittal plane in order to avoid unnecessary complexity regarding control and design. Moreover, it has been shown that for biped walking the dynamical effects in the lateral plane have a marginal influence on the dynamics in the sagittal plane. Key elements in the design phase were modularity and flexibility to be able to make changes to the robot configuration during the experimental process. This resulted in nearly the same mechanical and electronic configuration for each structural element such as lower leg, upper leg and body. These modular units are the same as the ones used for the pendulum structure. Six of these units are connected as depicted in Fig. 10. The same sensors, valve system and local microcontroller are provided for each unit. An additional micro-controller is used to read ground reaction force sensors, absolute position of the body and compressed air consumption. The high-level control is implemented on a PC. All the micro-controllers communicate with this central, Windows operated PC by a USB 2.0 serial

bus. As such, the complete biped is controlled at a sample rate of 2000Hz. The timing of the communication refresh rate is controlled by the USB Cypress micro-controller. One should also remark in the context of this refresh rate, that the delay time of the valves is about 1ms, which suggests that the communication frequency of 2000Hz is high enough. More information on the hardware of "Lucy" can be found in (Verrelst et al., 2005c).

5.2 Robot Control

The considered controller is given in the schematic overview on the right of Fig. 10 and is a combination of a global trajectory generator and a joint trajectory tracking controller. The trajectory generation is designed to generate walking movements based on objective locomotion parameters chosen for a specific robot step, which are average forward speed, step length, step height and intermediate foot lift. These parameters are calculated by a high level path planning control unit, which is beyond the scope of the current research. The trajectories of the leg links are represented by polynomials and are calculated by a simplified version of the method developed by Vermeulen (Vermeulen et al., 2005). The upper body and hip velocity is held constant in this case, which is valid for low walking speeds. In the future, the full method developed by Vermeulen will be used to achieve faster walking. The trajectories of the leg links, represented by polynomials, are planned in such a way that the upper body motion is naturally steered, meaning that in theory no ankle torque would be required. To overcome possible external disturbances, a polynomial reference trajectory is established for the upper body motion, which mimics a natural trajectory. Consequently the required ankle torque is low, meaning that it does not cause the ZMP (Zero Moment Point) to move out of the stability region. Thus, taking the motion of the upper body into account and not keeping it at a fixed angle as is the case in this paper. The effectiveness of this method applied to the robot "Lucy" has been proven in simulation (Verrelst et al., 2006).

The joint trajectory tracking controller is divided into three parts, analogously as for the pendulum structure: the computed torque module, the delta-p unit and the bang-bang pressure controller. The trajectory planner, computed torque module and delta-p unit are implemented on a central computer; the bang-bang controller on the micro-controllers.

After the trajectory generator the joint drive torques are calculated. This control unit is different for the single and double support phase. During single support the torques are calculated using the popular computed torque technique consisting of a feedforward part and a PID feedback loop. The same formulation is used as in equation (8), but the matrices D_e, C_e and G_e represent the complete robot. During single support the robot has 6 DoF and the 6 computed torques can be calculated straightforward. During the double support phase, immediately after the impact of the swing leg, however, three geometrical constraints are enforced on the motion of the system. They include the step length, step height and the angular position of the foot. Due to these constraints, the robot's DoF is reduced to 3. The dynamic model has to be reformulated in terms of the reduced independent variables. The dependant variables are related to the dependant variables through the kinematical Jacobian. An actuator redundancy arises because there are 6 actuators which need to control only 3 DoF. To be able to calculate the 6 joint drive torques, a control law as proposed by Shih (Shih et al., 1992) can be used, which is based on a matrix pseudo-inverse. The disadvantage is that these results are discontinue when switching between single and double support phase. A discussion on this implementation has been done by means of simulations (Verrelst et al., 2006). An alternative way to distribute torques over the actuators is to make a linear transition of torques between the old and new single support phase, by

calculating the applied torque as if the robot is in single support phase. The advantage of this strategy is that there are no torque discontinuities when switching between single and double support phase, but the calculated torques are not dynamical correct. However, the double support phase is rather short and a correcting feedback loop is provided. Experimental results show that this is a good strategy for the regarded motions.
The computed torque module presents all 6 required torque values to each local delta-p unit for each muscle pair of "Lucy". From this level on, the different control blocks are analogous to the one of the pendulum control structure. Of course, for each joint the specific torque generation characteristics are provided for the delta-p unit, since a hip, knee and ankle have different attachment points for the muscles. But in the current implementation the compliance strategy as used for the pendulum is not yet implemented for "Lucy", the compliance parameter is fixed at an arbitrary value.

5.3 Walking Experiments

In this section the measurements of the walking biped are shown with the following chosen objective locomotion parameters: mean forward velocity: 0.03m/s, steplength: 0.10m, stepheight: 0.0m, footlift: 0.04m. The calculated single support and double support phase durations are respectively 2.67s and 0.67s.
The graphs of Fig. 11 to Fig. 13 depict 4 double support phases and 4 single support phases. The graph at the left of Fig. 11 show the desired and real joint angles for the ankle, the knee and the hip. Vertical lines on all graphs show the phase transition instants. Due to the nature of the bang-bang pneumatic drive units and the imperfections introduced in the control loops, tracking errors can be observed. But tracking errors are not that stringent as it is for e.g. welding robots. The most important thing is that the overall dynamic robot stability is guaranteed. The graph on the right of Fig. 11 depicts the actual applied torque for the knee of the left leg, which consists of a PID feedback part and a computed torque part. The computed torque controller is working well, but the robot parameters still have to be fine-tuned to lower the action of the PID controller.

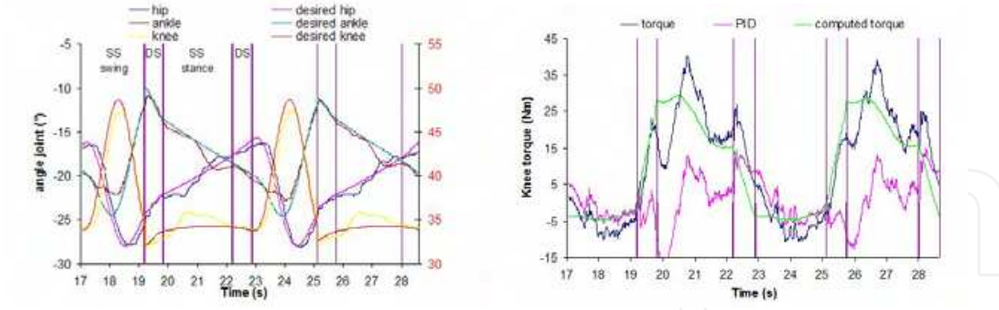


Fig. 11. (left) Desired and measured angle of left hip, knee and angle joint ; (right) Left knee torque.

The pneumatics are characterized by pressure courses in both muscles of each joint. The graphs in Fig. 12 show desired and measured gauge pressure for the front and rear muscle of the knee of the left leg. All these graphs additionally show the valve actions taken by the respective bang-bang pressure controller. Note that in these figures a muscle with closed valves is represented by a horizontal line depicted at the 2bar pressure level, while a small peak upwards represents one opened inlet valves, a small peak downwards one opened exhaust valves and the larger peaks represent two opened inlet or four opened outlet valves.

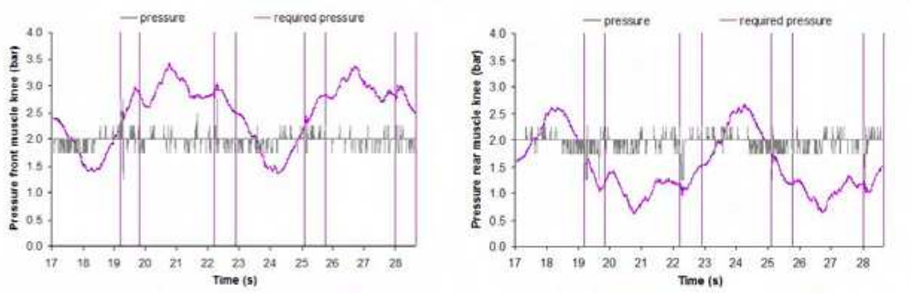


Fig. 12. Pressure and valve action of front (left) and rear (right) left knee muscle.

The desired pressures are calculated by the delta-p unit. For this experiment the mean pressure p_m (comparable to p_s) for all joints is taken at 2bar, consequently the sum of the pressures in each pair of graphs, drawing the front and rear muscle pressures, is always 4bar. It is observed that the bang-bang pressure controller is very adequate in tracking the desired pressure. Currently a lot of valve switching is required due to the fix compliance setting. By incorporating the natural dynamics of the system, as is described in the previous section, the switching will be reduced.

The two graphs in Fig. 13 depict the horizontal and vertical position of both feet as well as ZMP and CoG position.

Note that the swing foot moves twice the step length during the single support phase. Compared with the desired objective locomotion parameter, only small deviations can be observed. This proofs the global performance of the proposed trajectory control strategy. The position of the ZMP is measured by four load cells of Transducer Techniques (THA-250-Q). They are attached in the front and end of the sole plate and measure vertical ground forces, allowing to calculate the actual ZMP position in combination with the estimated ankle torques. Currently, the ZMP measurement is not used in the control loop yet, but it will be in the future to achieve faster walking. The ZMP and COG are close alike because the velocity of the robot is still rather slow. So the inertial influence is rather small compared to the gravitational component of the controller. The controller has however already performed well under dynamic walking situation in simulation (Verrelst et al., 2006). Several movies of the walking motion of the biped "lucy" can be seen at the following website: http://lucy.vub.ac.be.

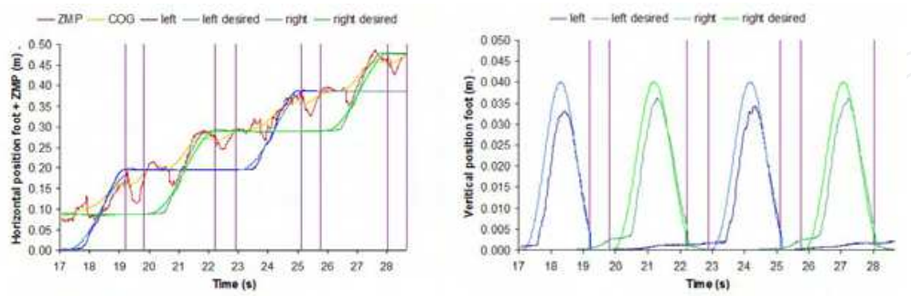


Fig. 13. (left) Horizontal position foot, Zero Moment Point (ZMP) and Centre of Gravity (COG) ; (right) Vertical position foot.

6. Conclusions

This publication discusses the importance of variable compliance for legged robots. Use of passive compliance in the actuation reduces reflected inertia which primarily is interesting

vis-à-vis safe human/robot interaction. But the variable compliance can also be used to change the natural dynamics of a system, which in turn can be exploited to reduce energy consumption of legged robots. Doing so, an interesting combination can be created between very energy efficient "passive walkers" and fully (stiffly) actuated versatile robots.
In the current state of our research the compliant actuation is provided with an antagonistic setup of pleated pneumatic artificial muscles. These specific muscles have been created to overcome some shortcomings of the more popular McKibben Artificial muscles. By regulating the both pressure in an antagonistic setup of two artificial muscles, as well as compliance as generated torque can be regulated. A description of the complete low-level tracking control is given, which includes a computed torque controller, a delta-p pressure calculation module, a bang-bang pressure controller and additionally a compliance controller. Most of these control blocks uses feedforward model based calculations.
The main purpose of the publication is to show that proper compliance control decreases energy consumption, which has been proven by simulation and experiments on a one DoF pendulum structure. The continuous compliance setting is applied for tracking a sine wave with varying frequency (shirp function), ranging from 1.5 to 2.0Hz. A comparison between proper and wrong compliance setting has been made with respect to estimated exergy consumption, which showed energy saving of more than six times, while the tracking output of the system is preserved. This clearly indicates the importance of variable compliance used for repetitive motion.
Finally, this repetitive motion is found in the movement of legged robots, which can be seen as an inverted pendulum motion for a stance leg and regular pendulum motion for a swing leg. As such the idea is to use the same compliance control of the pendulum structure for a bipedal walking robot. For this purpose the planar walking biped "Lucy", actuated by six pairs of artificial muscles, has been built. A short overview of the hardware and overall control system is given together with some basic walking experimental results. These results only discuss the tracking performance of the compliant actuation system and do not yet incorporate the proposed compliance control, which will be implemented in the near future. It is expected that the latter control structure substantially reduces energy consumption.
However, it has to be mentioned that the use of pneumatic energy in general is not energy efficient in an absolute sense. Thus, one should keep in mind that pneumatic energy for a mobile robot might not be the best solution, even if exploitation of natural dynamics is incorporated. Our research currently focuses on showing the importance of variable compliance for legged robots, in fact to show the relative decrease of energy consumption by proper compliance control. And, the current choice with the use of pneumatic artificial muscles provides a convenient way to implement this variable compliance. Parallel research is being conducted to develop alternative variable compliant actuation principles, by means of combining electrical actuation with standard passive spring elements. However, the developed trajectory tracking strategies, controlling the antagonistic setup with two artificial muscles, will be used for a compliant robotic exoskeleton to assist in the rehabilitation of paraplegic patients at the lower extremities. For such application energy consumption is not that stringent since the power source is used externally, but the compliant interface and the high power to weight ratio of the artificial muscles are extremely beneficial.

7. Bibliography

Asano, F., Yamkita, M. and Furuta, K. (2000). Virtual passive dynamic walking and energy-based control laws, *Proceedings of the IEEE/RSJ Int Conf on Intelligent Robots and Systems*, pp. 1149-1154.

Davis, S. T. and Caldwell, D. G. (2001). The bio-mimetic design of a robot primate using pneumatic artifcial muscle actuators, *Proc 4th Int Conf on Climbing and Walking Robots*, Karlsruhe, Germany, pp. 197-204.

Bicchi, A. and Tonietti, G. (2004). Fast and soft arm tactics: Dealing with the safety-performance trade-off in robot arms design and control, in *IEEE Robotics and Automation Magazine*, vol. 11, pp. 22-33.

Daerden, F. (1999). *Conception and Realization of Pleated Pneumatic Artifcial Muscles and their Use as Compliant Actuation Elements*, PhD thesis, Vrije Universiteit Brussel.

Daerden, F. and Lefeber, D. (2001). The concept and design of pleated pneumatic artifcial muscles., *International Journal of Fluid Power*, vol. 2, no. 3, pp. 41-50.

Garcia, M., Chatterjee, A., Ruina, A. and Coleman, M. (1998). The simplest walking model: Stability, complexity, and scaling, *ASME Journal of Biomechanical Engineering* 120: 281-288.

Gregorio, P., Ahmadi, M. and Buehler, M. (1997). Design, control, and energetics of an electrically actuated legged robot, *IEEE Transactions on Systems, Man and Cybernetics* 27B(4): 626-634.

Hollander, K.W. and Sugar, T.G. (2004). *Concepts for compliant actuation in wearable robotic systems*, US-Korea Conference, North Carolina, August.

Hurst, J. W., Chestnutt, J. and Rizzi, A. (2004), An actuator with physically variable stiffness for highly dynamic legged locomotion, new orleans, usa, pp. .," *Proc of the IEEE Int Conf on Robotics and Automation*, pp. 4662-4667.

International Standard ISO6358 (1989). Pneumatic fluid power - method of test - determination of flow rate characteristics of components using compressible fluids.

Lee, T.-T. and Liao, J.-H. (1988). Trajectory planning and control of a 3-link biped robot, *Proc. IEEE Int. Conf. on Robotics and Automation*, New York, USA, pp. 820-823.

Matsuoka, K. (1980). A mechanical model of repetitive hopping movements, *Biomechanisms* 5: 251-258.

McGeer, T. (1990). Passive dynamic walking, *Int. Journal of Robotics Research* 9(2): 62-82.

Migliore, S. A., Brown, E. A. and DeWeerth, S. P. (2005). Biologically inspired joint stiffness control, *Proc IEEE Int Conf on Robotics and Automation, Barcelona, Spain, April*, pp. 4519-4524.

Morita, T. and Sugano, S. (1995). Design and Development of a new Robot Joint using Mechanical Impedance Adjuster, *Proc IEEE Int Conf on Robotics and Automation,* Nagoya, Japan, *April*, pp. 2469-2475.

Okada, M., Nakamura, Y. and Ban, S (2001). Design of Programmable Passive Compliance Shoulder Mechanism, *Proc IEEE Int Conf on Robotics and Automation, Seoul, Korea, May*, pp. 348-353.

Osuka, K. and Saruta, Y. (2000). Development and control of new legged robot Quartet III - from active walking to passive walking, *Proc IEEE/RSJ Intl Conf on Intellegent Robots and Systems*, pp. 991-995.

Pratt, G. A. and Williamson, M. M. (1995). Series elastic actuators, *Proc IEEE-IROS Conference*, Pittsburg, USA, pp. 399-406.

Pratt, J. E. and Pratt, G. (1998). Exploiting natural dynamics in the control of a planar bipedal walking robot, *Proc of the 36th Annual Allerton Conf on Communication, Control, and Computing*, Monticello, Illinois.

Raibert, M. (1986). *Legged Robots That Balance*, MIT Press, Cambridge, Massachussetts.

Rogers, G. and Mayhew, Y. (1992). *Engineering Thermodynamics, Work and Heat Transfer*, John Wiley & Sons, New York, USA.

Sulzer, J., Peshkin, M. and Patton, J. (2005). Marionet: An exotendon-driven, rotary series elastic actuator for exerting joint torque, *Proc Int Conf on Robotics for Rehabilitation, Chicago, USA*.

Schulte, H. F. (1961). The characteristics of the McKibben artifcial muscle, *The Application of External Power in Prosthetics and Orthotics*, number Publication 874, National Academy of Sciences National Research Council, Lake Arrowhead, pp. 94-115.

Shih, C.-L. and Gruver, W. (1992). Control of a biped robot in the double-support phase, *IEEE Transactions on Systems, Man and Cybernetics* 22(4): 729-735.

Takanishi, A., Ishida, M., Yamazaki, Y. and Kato, I. (1985). The realization of dynamic walking by the biped walking robot WL-10RD, *Proc. Int. Conf. on Advanced Robotics*, pp. 459-466.

Thompson, C. and Raibert, M. (1989). Passive dynamic running, *Proceedings of the International Symposium of Experimental Robotics*, pp. 74-83.

M. Van Damme, R. Van Ham, B. Vanderborght, F. Daerden and D. Lefeber (2005). Design and Control of a "Soft" 2-DOF Planar Pneumatic Manipulator, *Proc. Int. Symp. on Measurement and Control in Robotics, Brussels, Belgium.*

van der Linde, R. Q. (1999). Design, analysis and control of a low power joint for walking robots, by phasic activation of mckibben muscles., *IEEE Transactions on Robotics and Automation* 15(4): 599-604.

Van Ham R., Vanderborght B., Van Damme M., Verrelst B., and Lefeber D (2005). MACCEPA: the Actuator with adaptable compliance for dynamic walking bipeds. *Proc 8th Int Conf on Climbing and Walking Robots, London, U.K., September*, pp. 759-766.

Van Ham, R., Verrelst, B., Daerden, F., Vanderborght, B., and Lefeber, D. (2005). Fast and accurate pressure control using on-off valves, *International Journal of Fluid Power*, vol. 6, March, pp. 53-58.

Vermeulen J., Verrelst B., Lefeber D., Kool P. & Vanderborght B. (2005). A real-time joint trajectory planner for dynamic walking bipeds in the sagittal plane, *Robotica,* Vol. 23, Issue 06, november, pp 669-680.

Verrelst, B., Van Ham, R. , Vanderborght, B., Vermeulen, J., Lefeber, D. and Daerden, F. (2005a). Exploiting adaptable passive behaviour to influence natural dynamics applied to legged robots, *Robotica*, vol. 23, no. 2, pp. 149-158.

Verrelst B., Vanderborght B., Vermeulen J., Van Ham R., Naudet J. & Lefeber D. (2005b). Control Architecture for the Pneumatically Actuated Dynamic Walking Biped "Lucy", *Mechatronics*, Volume 15, Issue 6, July, pp. 703-729.

Verrelst B., Van Ham R., Vanderborght B., Daerden F. & Lefeber D. (2005c). The Pneumatic Biped "LUCY" Actuated with Pleated Pneumatic Artificial Muscles, *Autonomous Robots,* vol.18, pp.201-213.

Verrelst B., Vermeulen J., Vanderborght B., Van Ham R., Naudet J., Lefeber D., Daerden F. & Van Damme M. (2006), Motion Generation and Control for the Pneumatic Biped "Lucy", *International Journal of Humanoid Robotics*, Vol. 3, No. 1, pp. 1-35.

Wisse, M. (2001). Biologically inspired biped design, *Symposium of the Int. Soc. for Postural and Gait Research*, Maastricht, The Netherlands, pp. 900-903.

Wisse, M., Schwab, A. L. and vd. Linde, R. Q. (2001). A 3d passive dynamic biped with yaw and roll compensation, *Robotica* 19: 275-284.

Yamguschi, J., Nishino, D. and Takanishi, A. (1998). Realization of dynamic biped walking varying joint stiffness using antagonistic driven joints, *Proc IEEE Int Conf on Robotics and Automatisation*, Leuven, Belgium, pp. 2022-2029.



Mobile Robotics, Moving Intelligence

Edited by Jonas Buchli

ISBN 3-86611-284-X

Hard cover, 586 pages

Publisher Pro Literatur Verlag, Germany / ARS, Austria

Published online 01, December, 2006

Published in print edition December, 2006

This book covers many aspects of the exciting research in mobile robotics. It deals with different aspects of the control problem, especially also under uncertainty and faults. Mechanical design issues are discussed along with new sensor and actuator concepts. Games like soccer are a good example which comprise many of the aforementioned challenges in a single comprehensive and in the same time entertaining framework. Thus, the book comprises contributions dealing with aspects of the Robotcup competition. The reader will get a feel how the problems cover virtually all engineering disciplines ranging from theoretical research to very application specific work. In addition interesting problems for physics and mathematics arises out of such research. We hope this book will be an inspiring source of knowledge and ideas, stimulating further research in this exciting field. The promises and possible benefits of such efforts are manifold, they range from new transportation systems, intelligent cars to flexible assistants in factories and construction sites, over service robot which assist and support us in daily live, all the way to the possibility for efficient help for impaired and advances in prosthetics.

How to reference

In order to correctly reference this scholarly work, feel free to copy and paste the following:

Bjorn Verrelst and Bram Vanderborght (2006). Novel Robotic Applications using Adaptable Compliant Actuation. An Implementation Towards Reduction of Energy Consumption for Legged Robots, Mobile Robotics, Moving Intelligence, Jonas Buchli (Ed.), ISBN: 3-86611-284-X, InTech, Available from: http://www.intechopen.com/books/mobile_robotics_moving_intelligence/novel_robotic_applications_using_adaptable_compliant_actuation__an_implementation_towards_reduction_

INTECH
open science | open minds

InTech Europe
University Campus STeP Ri
Slavka Krautzeka 83/A
51000 Rijeka, Croatia
Phone: +385 (51) 770 447
Fax: +385 (51) 686 166
www.intechopen.com

InTech China
Unit 405, Office Block, Hotel Equatorial Shanghai
No.65, Yan An Road (West), Shanghai, 200040, China
中国上海市延安西路65号上海国际贵都大饭店办公楼405单元
Phone: +86-21-62489820
Fax: +86-21-62489821

© 2006 The Author(s). Licensee IntechOpen. This chapter is distributed under the terms of the Creative Commons Attribution-NonCommercial-ShareAlike-3.0 License, which permits use, distribution and reproduction for non-commercial purposes, provided the original is properly cited and derivative works building on this content are distributed under the same license.

IntechOpen

IntechOpen